

Selective Aerobic Oxidation of 5-HMF into 2,5-Furandicarboxylic Acid with Pt Catalysts Supported on TiO₂- and ZrO₂-Based Supports

Hicham Ait Rass, Nadine Essayem, and Michèle Besson^{*[a]}

Pt catalysts prepared over different metallic oxide supports were investigated in the oxidation of 5-hydroxymethylfurfural (HMF) to 2,5-furandicarboxylic acid (FDCA) in alkaline aqueous solutions with air, to examine the combined effect of the support and base addition. The base (nature and amount) played a significant role in the degradation or oxidation of HMF. Increasing amounts of the weak NaHCO₃ base improved significantly the overall catalytic activity of Pt/TiO₂ and Pt/ZrO₂ by accelerating the oxidation steps, especially for the aldehyde group. This was highlighted by a proposed kinetic model that

gave very good concentration–time fittings. Moreover, the promotion of the catalyst with bismuth yielded a Pt–Bi/TiO₂ catalytic system with improved activity and stability. Y₂O₃– and La₂O₃–ZrO₂-supported catalysts exhibited lower activity than Pt/ZrO₂, which suggests no cooperative effect of the weakly basic properties introduced and the homogeneous base. Quantitative oxidation of HMF (0.1 M) and high yields of FDCA (>99%) were obtained in less than 5 h by using an HMF/Pt molar ratio of 100 and Na₂CO₃ as a weak base over Pt–Bi/TiO₂ (Bi/Pt=0.22).

Introduction

A shift from conventional petrochemical towards biomass-based feedstocks is of both environmental and economic importance for the future production of commodity chemicals.^[1,2] The most important plant-derived biomass sources with high potential are the carbohydrate components stored as polymers in biomass (starch, cellulose, or hemicellulose). Advances in the efficient transformation of these polymers give access to intermediate molecules that can be further converted into substitutes or analogues for chemicals currently obtained from petroleum.^[3,4]

One such analogue molecule is 2,5-furandicarboxylic acid (FDCA), the symmetrical furanic diacid synthesized from the key biobased precursor 5-hydroxymethylfurfural (HMF) through oxidation of both the primary alcohol and aldehyde groups. FDCA has been identified as a possible interesting substitute for terephthalic acid, a carbon fossil-based monomer used for polyester large-scale synthesis.^[4–7] The other important applications are expected to be for polyamides, polyurethanes, thermosets, and plasticizers.^[5,8] The HMF intermediate is accessible through acid-catalyzed dehydration of six-carbon carbohydrates, preferably from fructose rather than glucose.^[9,10]

Many of the common stoichiometric oxidation reagents have been used for the conversion of HMF to FDCA.^[11] Advantageously, the use of molecular oxygen is preferred over differ-

ent catalytic systems. Soluble metal bromide catalysts (Co/Mn/Br) in acetic acid, normally employed for the conventional oxidation of *para*-xylene to terephthalic acid, have been tailored for the HMF oxidation.^[12,13] Also, recoverable supported metallic nanoparticles, mainly Pt-,^[14–17] Ru-,^[18,19] and Au-based,^[20–24] and bimetallic catalysts^[25–27] that permit the reaction in an aqueous medium by using molecular oxygen or air have been investigated.

However, it is worth noting that the noble catalyst systems most often require an excess of a homogeneous base (mainly NaOH) that is larger than the molar stoichiometric amounts to accelerate the reaction and to maintain the FDCA formed in aqueous solution as the salt of the dicarboxylic acid; thus, the strong adsorption of the carboxylic acids on the catalyst is avoided. Even though some studies reported the possibility of conducting the aqueous-phase oxidation of HMF under base-free conditions by using basic solids such as hydrotalcites or mixed oxides (MgAl₂O₃, MgO–La₂O₃, etc.) as carrier materials for Ru(OH)_x or Au, it was demonstrated that these Mg-based supports dissolved extensively during the reaction and liberated detectable amounts of magnesium ions.^[18–20,28] In this case, the Mg-based solid bases served as a source of soluble basic species to make the mixtures alkaline and result in the formation of Mg–FDCA salts. On the other hand, the base-free oxidation of HMF over a Pt/ZrO₂ catalyst was also reported in a continuous flow system,^[16] HMF was completely converted with high selectivity for FDCA at *T*=100 °C and under a 10 bar pressure of air; a low liquid hourly space velocity (LHSV) of 3 h^{–1} was used for the conversion, and furthermore, a low concentration of HMF (0.5 wt%) was used to ensure full dissolution of the formed FDCA. Also, Pt nanoparticles stabilized by an ionic polymer were shown to catalyze the oxidation of HMF to

[a] H. Ait Rass, N. Essayem, M. Besson
IRCELYON, Institut de recherches sur la catalyse et l'environnement de Lyon
UMR5256 CNRS-Université Lyon 1
2 Avenue Albert Einstein, 69626 Villeurbanne Cedex (France)
Fax: (+33)0472445399
E-mail: michele.besson@ircelyon.univ-lyon1.fr

Supporting Information for this article is available on the WWW under
<http://dx.doi.org/10.1002/cssc.201403390>.

FDCA in water (HMF/Pt=20 at $T=80\text{ }^{\circ}\text{C}$ and $P=1\text{ bar O}_2$) without addition of a base.^[29] More recently, carbon nanotube (CNT)-supported Au–Pd catalysts achieved total HMF conversion with a yield of 94% FDCA in 12 h in water under base-free conditions ($T=100\text{ }^{\circ}\text{C}$ under $P=5\text{ bar O}_2$; HMF/(Au+Pd)=100).^[30] A stable Fe^{III}-polymer containing basic porphyrin subunits was proposed.^[31] It should be highlighted that, to be effective under base-free conditions, the catalysts must be loaded with a low HMF to metal molar ratio, typically in the range 20–40,^[18,29] or they require higher temperatures and longer reaction times compared with reactions performed with the addition of base.^[30] Even if it would be a more ecofriendly and safe to perform reactions in water, improved catalysts are still needed.

Some other results suggested that the catalyst support plays a role for the catalytic performances in this oxidation reaction. In the reaction at $T=65\text{ }^{\circ}\text{C}$ with 4 equivalents of NaOH under $P=10\text{ bar air}$ and an HMF/Au ratio of 150, Au/CeO₂ prepared by coprecipitation and a commercial Au/TiO₂ catalyst gave full HMF conversion with total selectivity to FDCA after 8 h, whereas Au/Fe₂O₃ and Au/C with similar Au dispersion were much less active.^[21] At $T=130\text{ }^{\circ}\text{C}$ (HMF/Au=640), the ceria support gave significantly fewer side products than the titania support. In the oxidation of HMF in alkaline aqueous solution at $T=90\text{ }^{\circ}\text{C}$ and under an atmospheric pressure of oxygen, the carrier ($\gamma\text{-Al}_2\text{O}_3$, TiO₂, ZrO₂–La₂O₃) used for supporting the preformed poly(*N*-vinyl-2-pyrrolidone) (PVP)-stabilized Pd nanoparticles influenced the yield of FDCA.^[31] The highest FDCA yield was obtained for a Pd/ZrO₂–La₂O₃ catalyst.

Different carbon types were also applied for supporting metals and the functional groups on the carbon atoms were found to have a crucial role.^[17,27,30,32] The rates of HMF oxidation were not influenced by the presence of acidic- or basic-site-functionalized carbon nanofibers (oxygen- or nitrogen-containing groups) in either the Pt or the Au case; however, the carbon-nanofiber support with basic groups improved the ability of supported Au to form FDCA from HMF under mild conditions.^[27] The carbonyl/quinone groups on functionalized carbon nanotubes supporting Au–Pd nanoparticles favored FDCA formation by enhancing adsorption of the reactant and intermediates, in contrast to carboxyl groups.^[30]

Recently, we also demonstrated that, in the presence of active-carbon-supported Pt catalysts, the use of 2 equivalents with respect to HMF of a milder base such as Na₂CO₃ in place of NaOH gave a very active catalyst with an excellent yield of FDCA by maintaining the desired optimum pH value during the oxidation of HMF in alkaline aqueous solution.^[17] In this study, we have investigated different oxide supports for Pt

that should be stable in aqueous solution (TiO₂, ZrO₂, and ZrO₂ in which Y₂O₃ or La₂O₃ was incorporated), and we examined the influence of the nature (NaHCO₃ or Na₂CO₃) and the amount of the homogeneous base on the catalytic performances of the resulting catalysts to evaluate whether lower amounts of homogeneous base could be used. Additionally, the possible promotion by bismuth and the recyclability have been studied for these new catalysts. Indeed, we have also previously shown a strong synergistic effect of Pt and Bi in terms of the activity and stability of a Bi-promoted catalyst relative to those of the monometallic Pt/C catalyst.^[17] Bi-promoted catalysts displayed superior activity compared with the monometallic catalyst, increased resistance to oxygen poisoning, and prevented Pt leaching. By using the optimized conditions ($T=100\text{ }^{\circ}\text{C}$, $P=40\text{ bar air}$, Na₂CO₃/HMF/Pt=2:1:0.01, and Bi/Pt=0.2), HMF was completely and selectively converted into FDCA within 3 h.

Results and Discussion

Characterization of catalysts

The chemical composition and physicochemical properties of the prepared Pt and Pt–Bi catalysts are listed in Table 1.

Table 1. Chemical composition and physicochemical parameters of the supports and supported Pt and Pt–Bi catalysts.

Catalyst	Metal loading [wt %]		BET surface area [m ² g ^{−1}]	Pore volume [cm ³ g ^{−1}]	Pore diameter [nm]	Metal particle size [nm]
	Pt	Bi				
TiO ₂	0	0	94	0.33	14	–
Pt/TiO ₂	3.6	0	92	0.32	13	2.2±0.6
Pt–Bi/TiO ₂	3.4	0.7	93	0.32	13	2.3±0.6
ZrO ₂	0	0	62	0.19	12	–
Pt/ZrO ₂	3.3	0	57	0.18	13	2.0±0.5
Pt–Bi/ZrO ₂	2.6	0.6	56	0.18	13	2.3±0.5
ZrO ₂ –La ₂ O ₃	0	0	133	0.25	7	–
Pt/ZrO ₂ –La ₂ O ₃	3.1	0	127	0.22	6	1.9±0.4
ZrO ₂ –Y ₂ O ₃	0	0	120	0.24	6	–
Pt/ZrO ₂ –Y ₂ O ₃	2.7	0	118	0.23	6	1.8±0.4

Doping of ZrO₂ with Y₂O₃ or La₂O₃ increased the specific surface area of the support. It increased the pore volume and decreased the average pore diameter from 12 nm in pure zirconia to 6 nm in the doped zirconia.

The surface areas and the pore volumes determined by N₂ physisorption of the bare supports and the corresponding Pt catalysts were in the same range. Moreover, deposition of Bi on the Pt catalyst did not produce a significant change in the total porosity. This indicates that the preparation methods that were chosen did not lead to significant changes in the physicochemical parameters of the bare supports.

X-ray diffraction patterns for the different Pt and Pt–Bi samples are shown in Figure S1 and Figure S2 in the Supporting Information. In all samples, only the typical patterns of the support (TiO₂ or ZrO₂) were observed, which suggests the presence of very small Pt crystallites (size < 2 nm). On titania, the X-

ray spectra showed broad peaks arising from the anatase phase. On pure zirconia, the most abundant phase was monoclinic. With incorporation of yttrium or lanthanum, zirconia was stabilized as the tetragonal phase with increases of the surface area and pore volume. In the X-ray patterns of the doped zirconia, no discernible reflections other than those of zirconia (tetragonal state) itself were observed. There was no diffraction from the La_2O_3 or Y_2O_3 crystallites, which indicated good dispersion or the formation of solid solutions.

Figure 1 shows representative micrographs from TEM analysis carried out on the TiO_2 -supported Pt and Pt–Bi catalysts.

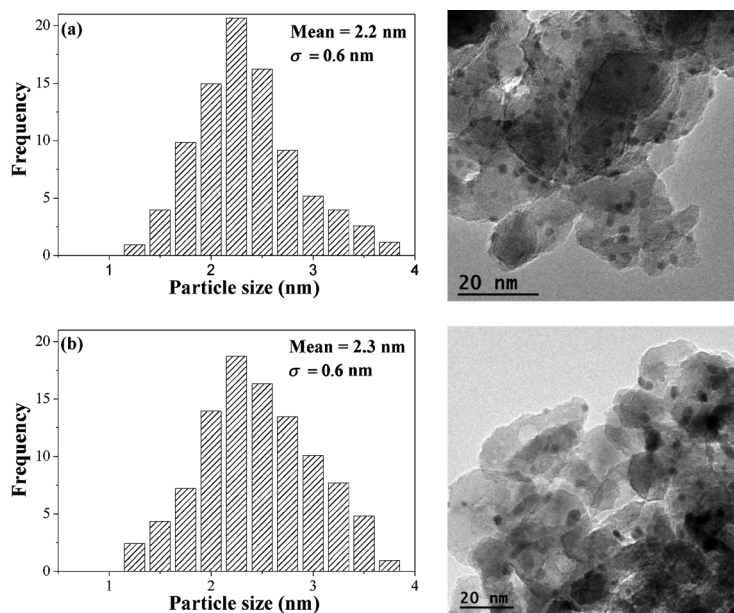


Figure 1. TEM images of catalysts and the corresponding particle size distributions: (a) 3.6% Pt/ TiO_2 ; (b) 3.4% Pt, 0.7% Bi/ TiO_2 .

The corresponding size distribution of the particles in each sample is also displayed. The TEM results for the ZrO_2 , ZrO_2 – La_2O_3 , and ZrO_2 – Y_2O_3 supported Pt (and Pt–Bi) catalysts are similarly shown in Figure S3 in the Supporting Information. In all solids, the support surfaces were uniformly covered with particles of relatively homogeneous sizes. The measurements for the Pt/ TiO_2 and Pt/ ZrO_2 catalysts revealed the presence of very small particles with the mean sizes estimated at (2.2 ± 0.6) and (2.0 ± 0.5) nm, respectively, with a quite narrow distribution. The mean particle sizes in the Pt/ ZrO_2 – La_2O_3 and Pt/ ZrO_2 – Y_2O_3 catalysts were slightly lower at (1.9 ± 0.4) and (1.8 ± 0.4) nm. In the Bi-promoted catalysts, the metal particles were also homogeneously distributed on the oxide supports. Figure 1b (3.4% Pt, 0.7% Bi/ TiO_2) and Figure S3b in the Supporting Information (2.6% Pt, 0.6% Bi/ ZrO_2) show that the deposition procedure of bismuth on the monometallic catalysts did not modify the average diameters, which were (2.3 ± 0.6) and (2.3 ± 0.5) nm, respectively. Energy-dispersive X-ray spectroscopy analysis of the bimetallic catalysts revealed that the particles contained both Pt and Bi with a molar ratio of approxi-

mately 0.2. Owing to the preparation method, it may be expected that the Bi lies mainly on top of the Pt.

Catalytic tests

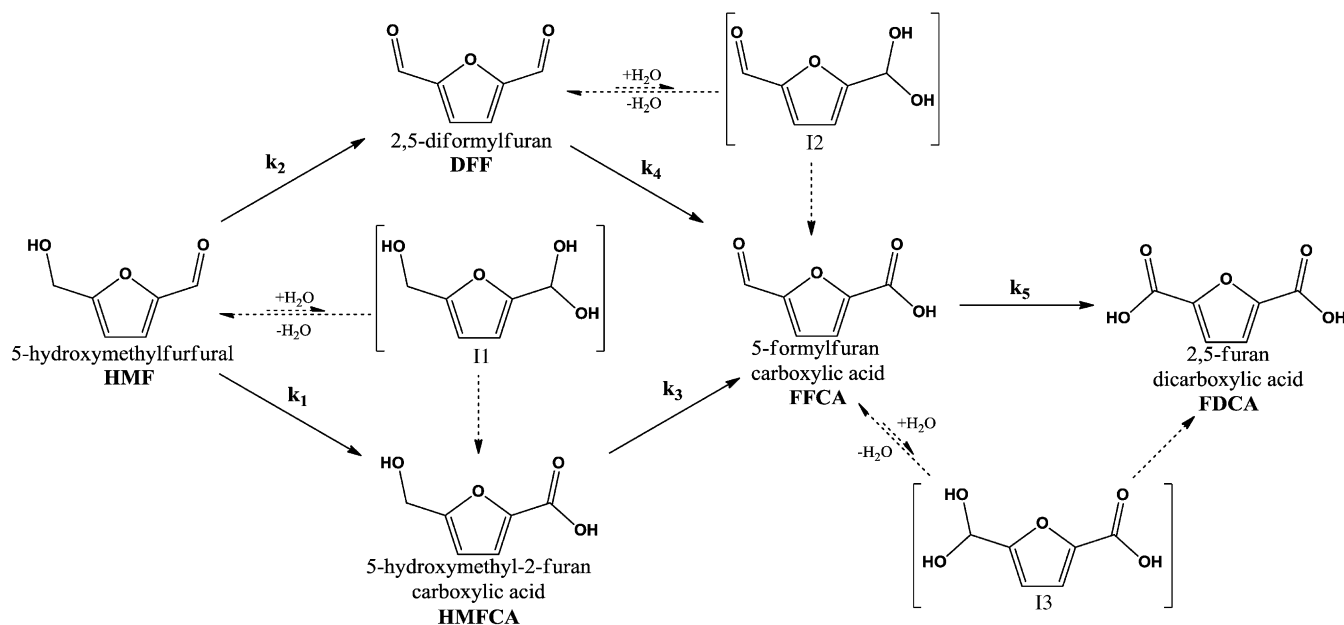
All catalysts listed in Table 1 were tested in the batch reactor under optimized test conditions: $T=100^\circ\text{C}$, $P=40$ bar air, 0.1 M HMF solution, and catalyst loading to give an HMF/Pt molar ratio of 100.

Modeling the reaction kinetics

The oxidation of HMF involves the oxidation of both the aldehyde and alcohol functional groups. By following the evolution of the reaction with time, different products were detected and analyzed. The catalytic oxidation of HMF to FDCA can be described by a mechanistic model, according to the pathway illustrated in Scheme 1.

The oxidation can proceed through the partially oxidized intermediates 5-hydroxymethyl-2-furancarboxylic acid (HMFCFA) and 2,5-diiformylfuran (DFF), which are both subsequently oxidized to 5-formyl-2-furancarboxylic acid (FFCA), before further oxidation to FDCA. It is generally believed that the hydroxymethyl group undergoes oxidative dehydrogenation to form the aldehyde and that the aldehyde groups are first hydrated to form the geminal diols (in I1, I2, and I3) before oxidative dehydrogenation to the acids.^[34–36] The base has been reported to enhance the selectivity towards carboxylic acids in the oxidation of alcohol or aldehyde functions, by favoring the conversion of the aldehyde into the corresponding geminal diol. The base also largely neutralizes the carboxylic acids responsible for product inhibition. Notably, oxygen participates indirectly in the reaction, by removing the adsorbed hydrogen atoms from the catalyst surface. In our study, the amount of oxygen introduced with $P=40$ bar air was estimated and found to be at least four times the amount required for the removal of hydrogen atoms adsorbed on the catalyst surface. Previous work has shown that the oxidation rates did not change beyond 40 bar air pressure, which indicated that O_2 availability at $P=40$ bar ($T=100^\circ\text{C}$) was not limiting for the complete oxidation of HMF to FDCA in this discontinuous batch mode reaction.

Moreover, the determination of the order of the reaction by using the differential method reveals that the HMF oxidation to DFF and HMFCFA is first order with respect to HMF. Elementary and nonelementary reaction rates were expressed from the proposed mechanistic model (Scheme 1) with the assumption that the first oxidation of HMF gives both DFF and HMFCFA. The rate equations for each species consumed and formed are given in Equations (1)–(5), in which k_i represents the various rate constants (Scheme 1) and C_w represents the concentrations of the various compounds.



Scheme 1. Reaction pathway for aqueous HMF oxidation to FDCA.

$$\frac{dC_{\text{HMF}}}{dt} = -(k_1 + k_2)C_{\text{HMF}} \quad (1)$$

$$\frac{dC_{\text{HMFA}}}{dt} = k_1C_{\text{HMF}} - k_3C_{\text{HMFA}} \quad (2)$$

$$\frac{dC_{\text{DFF}}}{dt} = k_2C_{\text{HMF}} - k_4C_{\text{DFF}} \quad (3)$$

$$\frac{dC_{\text{FFCA}}}{dt} = k_3C_{\text{HMFA}} + k_4C_{\text{DFF}} - k_5C_{\text{FFCA}} \quad (4)$$

$$\frac{dC_{\text{FDCA}}}{dt} = k_5C_{\text{FFCA}} \quad (5)$$

Modeling was performed in the MATLAB software. The least squares fitting algorithm of MATLAB *lsqcurvefit* was used to estimate the kinetic parameters of the different oxidation steps, with the assumptions that:

- 1) the temperature of the reaction is regulated and assumed to be stable throughout the experiment at 100 °C;
- 2) the amount of the active species of the catalyst is constant; that is, the catalyst undergoes no transformation during the catalytic reaction;
- 3) the *gem*-diol form of the aldehyde group is unstable and the equilibrium is shifted to carbonyl form;
- 4) all dehydrogenation reactions are irreversible;
- 5) the oxygen concentration is constant in the liquid phase and oxygen is sufficiently available.

Effect of the added base in blank tests

HMF is known to be unstable in alkaline aqueous solution.^[21,24,25,37] Background blank reactions were carried out in the absence of any catalyst to study the effects of time, the

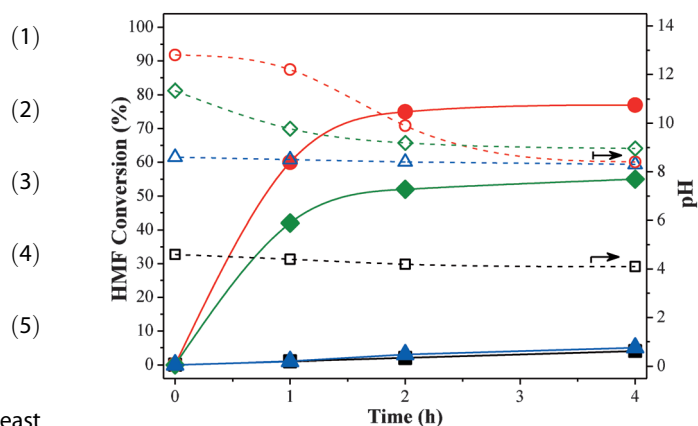
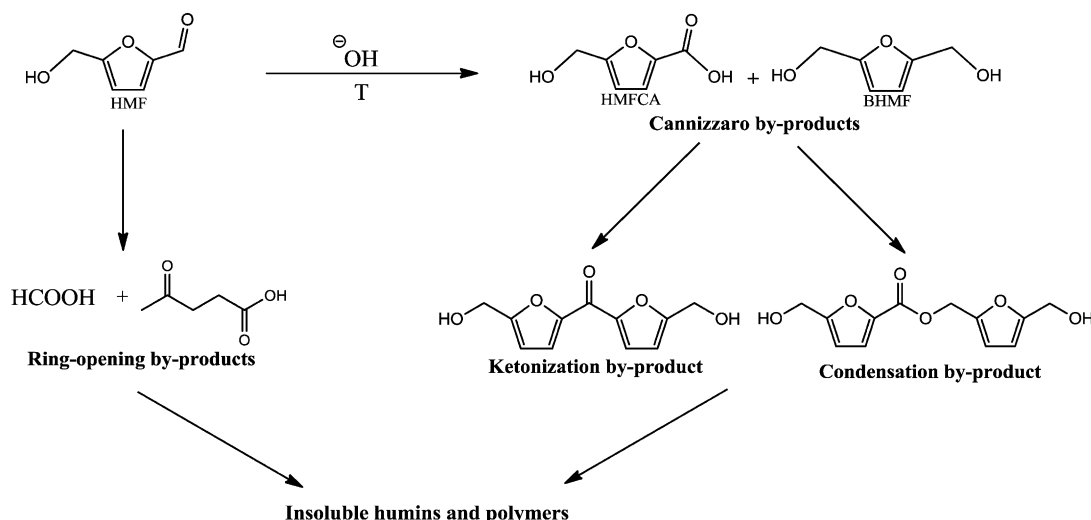


Figure 2. Degradation of HMF and evolution of the pH value, in a base-free aqueous solution or in the presence of different bases, without addition of a catalyst. Reaction conditions: no catalyst, $T = 100\text{ }^{\circ}\text{C}$, $P = 40\text{ bar air}$, 0.1 mol L^{-1} HMF. \square , \blacksquare : base-free; \triangle , \blacktriangle : 2 equiv NaHCO₃; \diamond , \blacklozenge : 2 equiv Na₂CO₃; \circ , \bullet : 2 equiv NaOH. Plain line and open symbol: HMF conversion; dotted line and filled symbol: pH value.

nature and amount of added base, and temperature on HMF stability under air pressure. Figure 2 shows the HMF conversion and the evolution of the pH value during the reaction. In the absence of base, HMF was found to be stable over time under standard conditions ($T = 100\text{ }^{\circ}\text{C}$, $P = 40\text{ bar air}$, and 0.1 mol L^{-1}). In the presence of NaOH (strong base) or Na₂CO₃ (weak base, $pK_s = 6.2$) with a base-to-HMF molar ratio of 2, HMF was rapidly degraded without the formation of the corresponding desired oxidation intermediates over 4 h (Scheme 2). The color of the reaction mixture turned rapidly from yellow to dark brown with longer reaction time. HPLC analysis detected HMFA and 2,5-bis(hydroxymethyl)furan (BHMF). Levulinic and formic acids could also be detected. However, these yields did not exceed 10% at the maximum after 1 h and then the concentrations



Scheme 2. Possible pathways of HMF degradation products during HMF oxidation at high temperature in the presence of strong added base.

decreased to yield humin byproducts, the structure of which must look like those described by van Zandvoort et al.^[38] The formation of these acids within the first one or two hours may explain why the pH value of the solution decreased at the beginning of the reaction.

In contrast, with the use of 2 equivalents of NaHCO₃ (weaker base, pK_a = 10.3), HMF was stable over time.

Analysis of the reaction medium clearly indicates that, at high pH values (pH > 11), HMF was degraded and the reaction pathway involved both ring opening to form levulinic acid and formic acid and the Cannizzaro reaction that leads to the formation of HMFCFA and BHMF by the base-induced disproportionation of the aldehyde group of HMF.^[39] The formation of products HMFCFA and BHMF with a maximum yield of 10% suggests that they reacted further to produce other waste products, as proposed in Scheme 2.

These results confirm that the pH value of the medium may be crucial for the oxidation reaction. Consequently, from these experiments, it can be suggested that HMF should be stable at pH values of less than 8. Operation at these pH values should minimize or suppress the formation of byproducts.

Influence of NaHCO₃ base content on the catalytic performances of Pt/TiO₂

The HMF oxidation reaction was carried out with the Pt/TiO₂ monometallic catalyst. Figure 3

shows the experimental and modeling results of 3.6% Pt/TiO₂ at different NaHCO₃-to-HMF molar ratios in the range 1–4 in comparison with the results of the base-free experiment.

First, under base-free conditions (Figure 3a), conversion of HMF was slow and was complete only after 12 h of reaction time. The major products formed during the reaction were DFF and FFCA, which confirmed that, in the absence of base, the oxidation occurs mainly by the oxidative dehydrogenation of the alcohol group of HMF to form the aldehyde (DFF). Indeed, it is accepted that, in the case of thermal activation under base-free conditions, the oxidation of the alcohol func-

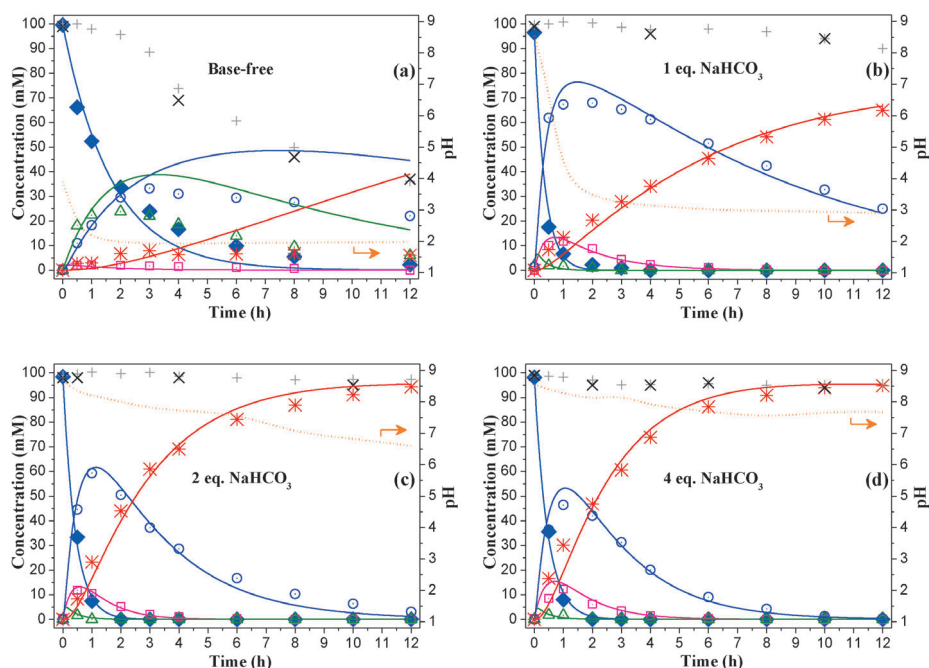


Figure 3. Evolution of the concentrations of HMF and the products DFF, HMFCFA, FFCA, and FDCA, as well as HPLC and TOC mass balances, as a function of time (experimental data: symbols; model estimates: lines) at different NaHCO₃/HMF molar ratios in the presence of 3.6% Pt/TiO₂: (a) 0 equiv NaHCO₃; (b) 1 equiv NaHCO₃; (c) 2 equiv NaHCO₃; (d) 4 equiv NaHCO₃. Reaction conditions: T = 100 °C, P = 40 bar air, 0.1 M HMF, HMF-to-Pt molar ratio = 100. ◆: HMF; △: DFF; □: HMFCFA; ○: FFCA; * : FDCA; +: molar balance; ×: TOC;: pH value.

tion is the rate-controlling step of the HMF oxidation.^[14] The oxidation rate of the aldehyde functional groups in the two intermediates is very low, as a result of the acidic medium, which is unfavorable for the initial hydration of the aldehyde to the *gem*-diol. A high defect in the molar balance was rapidly observed (40–50%, both by HPLC and total organic carbon (TOC) measurements), which is attributed to precipitation of the acids and diacid formed onto the catalyst surface. Indeed, FDCA, FFCA, and HMFCa are water-insoluble compounds (≈ 0.09 wt% solubility of FDCA in water at $T = 30^\circ\text{C}$).^[16] The crystallization is favored by a low pH value of the aqueous medium ($\text{pH} < 2$) in the absence of a base and it decreases the reaction rate.

The used catalysts were analyzed to confirm the deposition of products on the solids. Figure 4 shows the thermogravimetric

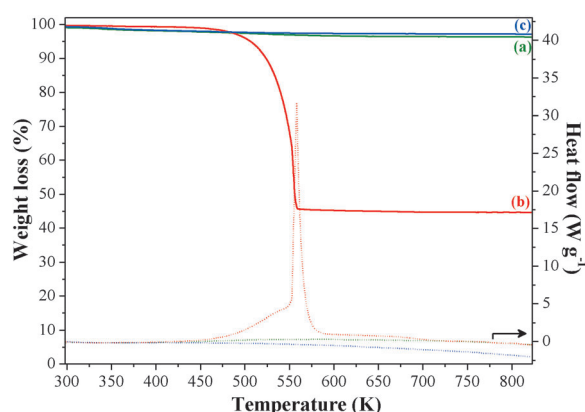


Figure 4. TG analysis (solid line) and differential thermal analysis (dotted line) in air of 3.6% Pt/TiO₂ (a) before (—), (b) after catalytic testing in base-free conditions (—), and c) after catalytic testing in the presence of 2 equivalents of NaHCO₃ (—).

ric analysis (TGA) and compares the weight loss for the fresh catalyst and the solids recovered after catalytic tests in the absence or presence of base. The minor weight loss observed for fresh catalyst and the used catalyst in the presence of a base corresponds to the release of absorbed water, whereas a significant weight loss ($> 50\%$) was observed between $T = 150$ and 300°C for the used catalyst under base-free conditions; this loss can be assigned to the decomposition of adsorbed furanic compounds on the catalyst surface, most likely solid carboxylic acids recovered with the used catalyst.

The solubility of the carboxylic compounds can be improved by forming the carboxylate salts by addition of a base (preferentially a weak base). For one mole of FDCA, two moles of sodium ions are required to generate the 2,5-furan dicarboxylate ion. It is evident that, in the presence of increasing amounts of NaHCO₃ homogeneous base (Figure 3 b,c,d), oxidation rates were improved relative to those in base-free conditions. In all cases, HMF was nearly completely converted within 2 h. HMFCa and FFCA were formed as major intermediates and much better molar balances (95–100%) were attained, which demonstrated the pivotal role of the added homogeneous base.

In the presence of one molar equivalent of NaHCO₃ (0.5 equiv Na⁺), the FFCA yield attained a maximum of 70% when the HMF had been completely consumed after 2 h. This maximum concentration decreased to 60% and 40% as the molar ratio of NaHCO₃ to HMF increased to 2 and 4, respectively. In fact, the increasing base loading (which influences the pH value of the reaction medium) accelerated drastically the rate of the subsequent oxidation of FFCA to FDCA. If only half the amount of base required to neutralize the diacid was added (NaHCO₃/HMF = 1), the pH value of the reaction medium dropped from 9 to 3 as the reaction proceeded, and the reaction was not completed after 12 h of reaction (Figure 3 b). The final oxidation of FFCA was still low as a result of the acidic medium and a 10% loss in molar balance was noted after 12 h, which we attribute to crystallization of FDCA. If the reaction was followed for up to 24 h, the loss increased to 25% (not shown). With 2 equivalents of base (the stoichiometric amount required to neutralize the acid groups of FDCA formed), the final pH value was 6.7 and FFCA was totally converted into FDCA after 12 h (Figure 3 c). However, after a further increase of the base concentration (NaHCO₃/HMF = 4), the pH value remained above 7.6 and a yield of FDCA $> 95\%$ was attained within 10 h (Figure 3 d). This can be explained by the acceleration of the hydration of aldehydes in the aqueous solution to geminal diols by the base. However, a slight loss in the mass balance, based both on the HPLC-detected products and TOC analysis, was observed in the presence of 4 equivalents of NaHCO₃ (Figure 3 d), whereas it was nearly complete at the lower NaHCO₃/HMF ratio of 2 (Figure 3 c). Therefore, we suggest that the optimum NaHCO₃-to-HMF molar ratio would rather be 2 in the presence of Pt/TiO₂ catalyst. In our previous work with a Pt/C catalyst, 4 equivalents of NaHCO₃ were shown to be necessary.^[17] Similar catalytic performances to those of Pt/C can be obtained with Pt/TiO₂, although a NaHCO₃/HMF ratio of 2 instead of 4 for Pt/C is sufficient.

The oxidation rate constants for the chosen model were estimated from the experimental kinetic data (represented by symbols in Figure 3), through least squares parameter fitting by minimizing the sum of the squared error between the experimental concentration values and the concentration values calculated by the system of first-order ordinary differential equations. The estimated kinetic parameters are given in Table 2.

In the base-free reaction, after a good fitting during the early phase of oxidation of HMF, a significant gap was observed after 1 h between the experimental and estimated data,

Table 2. Kinetic parameters estimated for the 3.6% Pt/TiO ₂ catalyst.					
Amount of added base	Rate constant [h ⁻¹]				
	k_1	k_2	k_3	k_4	k_5
base-free reaction	0.244	0.351	8.031	0.125	0.080
1 equiv NaHCO ₃	0.596	2.208	0.604	24.781	0.129
2 equiv NaHCO ₃	0.616	1.771	1.139	27.334	0.397
4 equiv NaHCO ₃	0.618	1.590	0.831	27.444	0.525
2 equiv Na ₂ CO ₃	1.643	1.897	0.904	74.154	1.412

which is the logical consequence of byproduct formation and leads to the dramatic increase of defect in the molar balances (Figure 3 a).

In opposition to what was observed in the base-free reaction, the results in Figure 3b, c, and d indicate that, with the addition of the base NaHCO_3 , a close match was obtained within the entire range of time between the experimental and estimated concentrations versus time data. This shows that the model described in Scheme 1 represents a good approximation for the conversion of HMF into FDCA. The mechanism of oxidation of aldehyde to carboxylic acid involves a base-catalyzed hydration of aldehyde to geminal diol. According to the calculated kinetic constants, and as expected from this mechanism, increasing amounts of base not only neutralize the carboxylic functions but also accelerate the oxidation rates of the aldehyde functions in the intermediates to the fully oxidized FDCA (k_4 and particularly k_5). The model provides higher values for k_2 than for k_1 , which would suggest the predominant formation of the DFF intermediate. However, one must consider that the aldehyde function reacts very rapidly in the presence of the base to yield FFCA and the maximum amount of DFF formed is very low. This is consistent with the high reactivity of DFF demonstrated by Verdeguer et al.,^[15] who measured a turnover frequency of 48 h^{-1} for DFF compared with 4 h^{-1} for HMF. In the presence of 4 equivalents of NaHCO_3 , the constant k_5 , which determines the rate of transformation of FFCA to FDCA, exhibits a four-times higher value than that with the use of 1 equivalent of NaHCO_3 .

Effect of using Na_2CO_3 base for Pt/TiO₂

As previously studied with a Pt/C catalyst,^[17] the influence of the nature of the carbonate base (CO_3^{2-} versus HCO_3^- , $\text{p}K_b = 3.65$ and 7.65 , respectively) was studied over the 3.6% Pt/TiO₂ catalyst. The substitution of 4 equivalents of NaHCO_3 by 2 equivalents of Na_2CO_3 improved significantly all oxidation rates, as shown in Figure 5. The reaction was completed within 8 h with a final yield of FDCA of 91%. The effect was as shown previously in the presence of Pt/C; that is, the addition of 2 equivalents of carbonate with respect to HMF increased significantly the overall oxidation rate compared to the use of 4 equivalents of bicarbonate. These rate increases are essentially due to the pH value, which remains at a value of more than 8 throughout the oxidation reaction.

As compared with the reaction with 4 equivalents of NaHCO_3 , it was also noted that the yield of the intermediate oxidation product HMFCa was significantly increased at the initial reaction stage in the presence of 2 equivalents of Na_2CO_3 . HMFCa was formed in a maximum concentration of 30 mmol L^{-1} after 30 min. The HMFCa and FFCA maximum concentrations were formed in almost the same amount. This is different to the reactions performed in the presence of NaHCO_3 , in which both HMFCa and DFF were observed in small amounts. Also, no intermediate product DFF was detected during the reaction with Na_2CO_3 as the base. Moreover, the HPLC and TOC balances did not fit. A defect in balance based on HPLC analysis was noted, whereas the TOC balance was

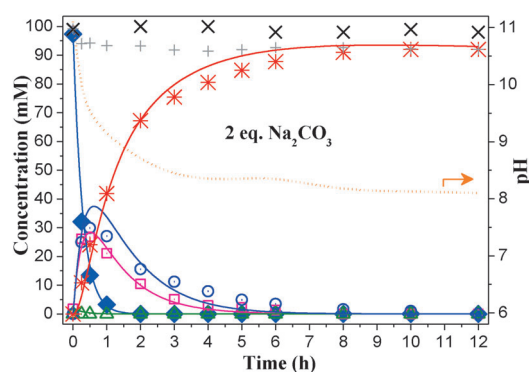


Figure 5. Evolution of the concentrations of HMF and the products DFF, HMFCa, FFCA, and FDCA as a function of time (experimental data: symbols; model estimates: lines) over 3.6% Pt/TiO₂ in the presence of Na_2CO_3 . Reaction conditions: $T = 100^\circ\text{C}$, $P = 40 \text{ bar}$ air, 0.1 M HMF, HMF-to-Pt molar ratio = 100, $\text{Na}_2\text{CO}_3/\text{HMF} = 2$. \blacklozenge : HMF; \blacktriangle : DFF; \square : HMFCa; \circ : FFCA; $*$: FDCA; $+$: molar balance; \times : TOC; \cdots : pH value.

complete over the entire course of the reaction. This indicates that some waste products are formed under these basic conditions that are not detected by HPLC; however, they are soluble and not adsorbed on the solid catalyst. As mentioned previously (Scheme 2), under strong basic conditions (which seems to be the case with 2 equivalents of Na_2CO_3), HMF degradation occurs through the Cannizzaro reaction disproportionation to form HMFCa. Furthermore, under too basic conditions, HMFCa is also not stable and degradation of HMFCa can take place. In addition, the absence of DFF might be due to the basic medium favoring the Cannizzaro reaction of DFF. These results confirm that a moderately basic reaction medium is preferable for the Pt/TiO₂ catalyst. The substrate HMF and the first intermediates formed seem to be more sensitive to the basicity of the reaction medium in the presence of Pt/TiO₂ than Pt/C.

The kinetic constants in the presence of 2 equivalents of Na_2CO_3 differ from those obtained with 4 equivalents of NaHCO_3 (Table 2). The oxidation reactions of the aldehyde functions in the reactant and in the intermediates were drastically accelerated, as demonstrated by the larger values of the k_1 , k_4 , and k_5 constants, which were multiplied by around a threefold factor. In particular, there was a significant acceleration in the final oxidation of FFCA to FDCA. In contrast, the k_2 and k_3 constants that correspond to the oxidation of an alcohol function increased little. The higher performance of the catalyst with the addition of 2 equivalents of the CO_3^{2-} base compared with 4 equivalents of HCO_3^- base can be explained by the strength of these bases.^[40]

Analysis of the final reaction mixtures by inductively coupled plasma optical emission spectroscopy (ICP-OES) showed that a small amount of the platinum metal was leached (up to 3%).

Effect of the nature of the oxide support

The supports ZrO_2 , $\text{Y}_2\text{O}_3\text{-ZrO}_2$, and $\text{La}_2\text{O}_3\text{-ZrO}_2$ were used to evaluate if the basic sites introduced in ZrO_2 could cooperate with the homogeneous base and allow the amount of added base to be reduced. Catalytic experiments of the zirconia-

based Pt catalysts were carried out under the optimum reaction conditions determined for Pt/TiO₂ ($T=100^{\circ}\text{C}$, 40 bar air pressure, and HMF/Pt=100) in the presence of 2 equivalents of NaHCO₃. The results are summarized in Table 3.

Table 3. Comparison of the catalytic performances of Pt supported on different zirconia supports in the presence of NaHCO₃ (NaHCO₃/HMF=2) after 2, 12, and 24 h.^[a]

Catalyst	2 h		12 h		24 h	
	HMF conv. [%]	FFCA yield [%]	FDCA yield [%]	FFCA yield [%]	FDCA yield [%]	FDCA yield [%]
Pt/ZrO ₂	97	13	82	0	95	
Pt/ZrO ₂ -Y ₂ O ₃	91	29 ^[b]	63	15	78	
Pt/ZrO ₂ -La ₂ O ₃	74	37 ^[c]	56	18	75	

[a] Reaction conditions: $T=100^{\circ}\text{C}$, $P=40$ bar air, 0.1 M HMF, HMF-to-Pt molar ratio=100, NaHCO₃/HMF=2. [b] Contains also 2% of HMFCFA. [c] Contains also 7% of HMFCFA.

As seen from Table 3, Pt/ZrO₂ exhibited lower performances in comparison with Pt/TiO₂ under the same conditions. Conversion of HMF was complete in more than 2 h. The partially oxidized intermediates HMFCFA and DFF formed in small amounts were rapidly oxidized to FFCA. After 24 h, 95% of FDCA was obtained over Pt/ZrO₂. It is expected that the doping of ZrO₂ with Y₂O₃ or La₂O₃ will introduce some basicity in the catalyst.^[41,42] However, the results indicate that the doping did not improve the catalytic activity of the Pt catalysts. Yields of FDCA of 78 and 75% were obtained in the presence of Pt/ZrO₂-Y₂O₃ and Pt/ZrO₂-La₂O₃, respectively. Hence, if we consider that the Pt dispersion was very similar in all ZrO₂-based catalysts (Figure 1 and Figure S3 in the Supporting Information), the introduction of Y₂O₃ or La₂O₃ even decreased the oxidation efficiency of Pt/ZrO₂. These observations are different from the results of Siyo et al. for Pd catalysts. They obtained higher yields in FDCA in the presence of Pd-nanoparticles/ZrO₂-La₂O₃ than in the presence of Pd-nanoparticles deposited on TiO₂.^[32]

Small defects of molar balance (< 5%) were always observed in the presence of Pt supported on zirconia-based supports. Analysis of the final reaction mixtures revealed that after 24 h about 3% Pt had leached from the catalysts, as with Pt/TiO₂.

Catalytic experiments over these catalysts were also conducted under base-free conditions. The catalysts displayed very low activity; HMF conversion was slow and was not complete after 24 h (80% HMF conversion). The major intermediates observed were DFF (20%) and FFCA (25%). In the presence of Pt/ZrO₂, only 10% of FDCA was formed after 24 h. This low productivity is in line with the results of Lilga et al.,^[16] who had to use a large catalyst/HMF ratio.

The influence of the nature of the added base with Pt/ZrO₂ was also studied, and the results with 2 equivalents of NaHCO₃ or Na₂CO₃ (2 and 4 equiv Na⁺, respectively) are compared in Figure 6. The addition of Na₂CO₃ in place of NaHCO₃ improved significantly the oxidation rates and maintained the higher pH value (> 8). As for Pt/TiO₂, with Na₂CO₃, HMF was fully oxidized after 1 h and 93% of FDCA was reached in less than 10 h, relative to more than 24 h with NaHCO₃. There was a small dis-

crepancy in the mass balance on the HPLC-detected products and the TOC balance in both experiments in the presence of Pt/ZrO₂.

Stability of catalysts

The recyclability and stability of the Pt/TiO₂ catalyst was investigated by reusing the catalyst in consecutive catalytic runs. Figure 7 compares the evolution at total conversion of HMF of the selectivities to FFCA and FDCA for four successive runs after 12 h under the optimized reaction conditions ($T=100^{\circ}\text{C}$, $P=40$ bar air, HMF/Pt=100) in the presence of 2 equivalents of NaHCO₃.

In the first run (Figure 7), HMF was fully oxidized in less than 2 h and a nearly complete conversion to FDCA was attained after 12 h. After the first run, the spent catalyst was simply recovered by filtration, washed with water, and dried overnight under vacuum at 40 °C. When the spent catalyst was reused without any reactivation (second and third runs), a significant decrease of activity was observed. Indeed, total oxidation of HMF was attained after 4 h, and the amount of unconverted FFCA increased in the second and again in the third runs. The reaction mixture analyzed by ICP-OES at the end of the experiments revealed that very small quantities of Pt (< 2%) were leached out in the solution, which cannot explain the deactivation. The

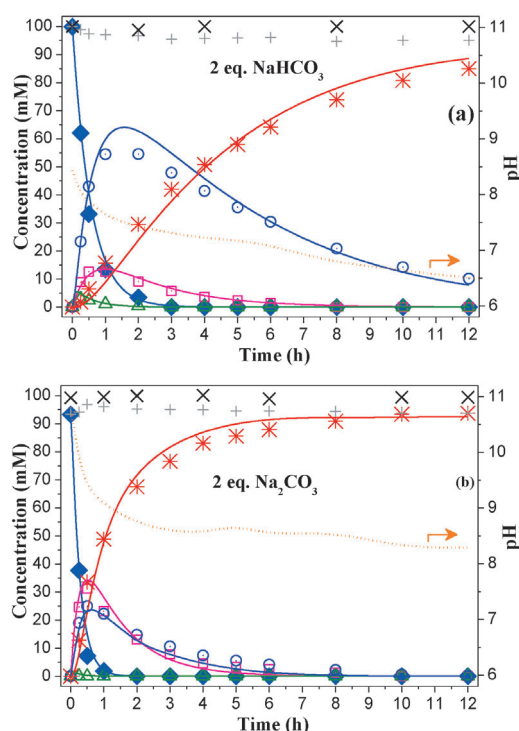


Figure 6. Effect of the nature of the base (Na₂CO₃ versus NaHCO₃) in the oxidation of HMF (experimental data: symbols; model estimates: lines) with Pt/ZrO₂: (a) NaHCO₃ and (b) Na₂CO₃. Reaction conditions: $T=100^{\circ}\text{C}$, $P=40$ bar air, 0.1 M HMF, HMF-to-Pt molar ratio=100. ◆: HMF; △: DFF; □: HMFCFA; ○: FFCA; * : FDCA; + : molar balance; x : TOC; ● : pH value.

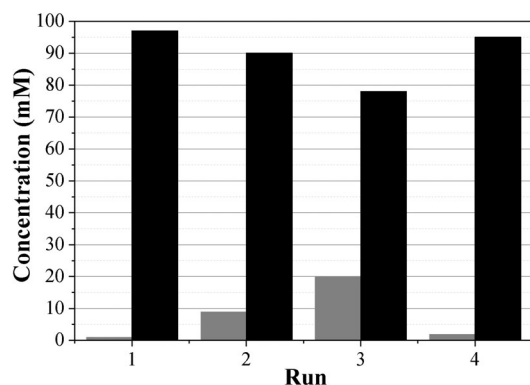


Figure 7. Consecutive use of Pt/TiO₂ (■: FDCA; ▨: FFCA): 1st run: fresh catalyst; 2nd and 3rd runs: spent catalyst used without reactivation; 4th run: catalyst used after reduction of the spent catalyst. Reaction conditions: $T = 100\text{ }^{\circ}\text{C}$, $P = 40\text{ bar}$ air, 0.1 M HMF, HMF-to-Pt molar ratio = 100, $\text{NaHCO}_3/\text{HMF} = 2$, $t = 12\text{ h}$.

catalyst recovered after the third run was reactivated by reduction under hydrogen. The initial catalytic activity was then totally recovered (run 4). This behavior was also observed during HMF oxidation over Pt supported on carbon, for which the oxygen atmosphere led to covering by oxygen or overoxidation of the active platinum sites during catalytic tests when HMF was fully converted.^[17]

A solution to this problem proposed in the literature for the oxidation of alcohols or carbonyl compounds in aqueous solution is the addition of another metal, such as bismuth (a non-noble metal). Bi can protect the platinum from oxidation, and the oxophilic properties promote the oxidative dehydrogenation of the alcohol group by interaction between Bi and a π electron of the furan ring.^[17] If used alone, bismuth is inactive for the oxidation reaction; if associated to Pt, a significant increase of the overall catalytic performances and lifetime of the catalyst was observed in HMF oxidation with Pt supported on carbon. Bi promotion also limited Pt leaching into the reaction medium.

Therefore, we prepared bimetallic Pt–Bi/TiO₂ catalysts with different Bi/Pt ratios varying between 0.09 and 0.52. Table 4 compares the catalytic performances of the Pt/TiO₂ catalysts loaded with different Bi/Pt molar ratios after 1 and 6 h of reaction for HMF conversion and for HMFCa, FFCA, and FDCA formation. The reaction was performed under standard conditions

Table 4. Comparison of the catalytic performances after 1 and 6 h of the reaction of bismuth-promoted Pt/TiO₂ with varying Bi/Pt molar ratios by using Na₂CO₃ (Na₂CO₃/HMF = 2).

Bi/Pt	1 h		6 h			Rate constant [h ⁻¹]				
	conv. [%]		yield [%]			k_1	k_2	k_3	k_4	k_5
	HMF		HMFCa	FFCA	FDCA					
0	90	<1	6	84		0.637	0.953	0.433	10.119	1.374
0.09	99	1	2	94		0.467	2.246	0.370	20.820	3.208
0.22	>99	0	0	99		0.876	3.656	0.820	49.181	3.605
0.32	>99	0	1	97		0.410	3.264	0.514	25.342	3.452
0.52	95	3	8	84		0.898	1.426	0.489	24.354	1.179

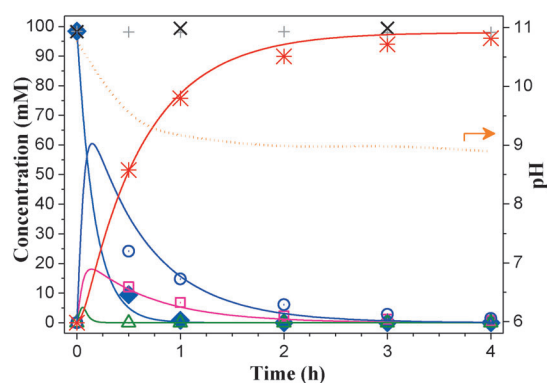


Figure 8. Evolution of the concentrations of HMF and the products DFF, HMFCa, FFCA, and FDCA as a function of time (experimental data: symbols; model estimates: lines) over Pt–Bi/TiO₂ (Bi/Pt = 0.22) in the presence of 2 equivalents of Na₂CO₃. Reaction conditions: $T = 100\text{ }^{\circ}\text{C}$, $P = 40\text{ bar}$ air, 0.1 M HMF, HMF-to-Pt molar ratio = 100, Na₂CO₃/HMF = 2. ◆: HMF; △: DFF; □: HMFCa; ○: FFCA; * : FDCA; + : molar balance; x : TOC;: pH value.

with 2 equivalents of Na₂CO₃. The course of the reaction as a function of reaction time is illustrated in Figure 8 for the Bi/Pt molar ratio of 0.22.

The oxidation of HMF in the presence of Pt/TiO₂ promoted by bismuth was remarkably accelerated with respect to the monometallic parent catalyst up to a Bi/Pt ratio of around 0.22. With this 0.22 ratio, total conversion of HMF was attained after 1 h and FFCA formed was completely converted into FDCA in less than 4 h, compared with more than 8 h without Bi promotion (Figure 8 versus Figure 6b). A good molar balance was calculated, which was improved relative to that of the experiments on the monometallic catalysts. The solutions that were yellow in the presence of the Pt/TiO₂ catalyst became colorless when Bi was added. A further increase of the Bi/Pt ratio to 0.32 did not change significantly the overall reaction rate, and the balances were still complete. However, higher bismuth loading (Bi/Pt = 0.52) led to a loss of the beneficial effect of Bi promotion as a result of high coverages of the Pt particles with Bi, based on the knowledge that it is deposited on top of the metallic surface. At the end of the 6 h reaction, the final yield of FDCA was 84%, which is similar to that obtained over the nonpromoted catalyst.

With regard to the kinetic constants deduced from the model, they show the synergistic effect brought by Bi promotion up to the optimum Bi/Pt ratio of 0.2–0.3. Nevertheless, the effect is not as significant as that observed for Pt/C catalysts for this reaction under the same reaction conditions.^[17]

The promoted 2.6 wt% Pt–0.6 wt% Bi/ZrO₂ catalyst (molar ratio Bi/Pt = 0.25) was compared with the monometallic counterpart with 2 equivalents of Na₂CO₃. A similar synergistic effect of Bi was observed: total oxidation of HMF and the intermediates was complete after 6 h with a yield of FDCA of 97%, instead of 10 h and a yield of 93% in the presence of Pt/ZrO₂. The mass balances were in relatively good agreement.

Analysis of the filtered reaction medium by ICP-OES after the reaction showed no detectable leaching of Pt (Pt < 0.5%) in contrast to the monometallic catalyst (Pt ≈ 3%) and no bismuth leaching (Bi < 0.5%). In addition to the stabilization of

the metallic active sites, the promotion by Bi also lowers the leaching of the Pt surface.

Bimetallic catalyst recyclability was also investigated by reusing the Pt–Bi/TiO₂ catalyst with a Bi/Pt ratio of 0.22 in consecutive runs. The results for four runs are shown in Figure 9. It

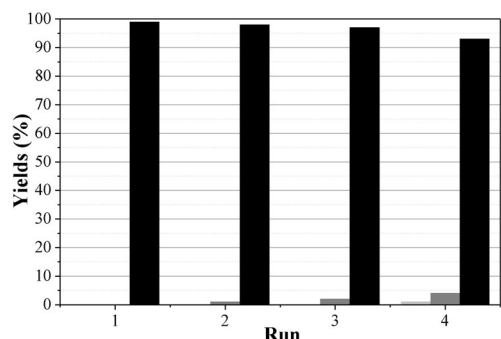


Figure 9. Successive reuse of Pt–Bi/TiO₂ (Bi/Pt molar ratio = 0.22) without pretreatment of the spent catalyst. Reaction conditions: $T = 100\text{ }^{\circ}\text{C}$, $P = 40\text{ bar}$ air, 0.1 M HMF, HMF-to-Pt molar ratio = 100, $\text{Na}_2\text{CO}_3/\text{HMF} = 2$, $t = 10\text{ h}$. ■: HMFCa; ■: FFCA; ■: FDCA.

must be emphasized that, in this case, the recovered catalyst has not been reactivated under H₂ after each run. It was just filtered off the solution of the previous run carried out over 10 h of reaction, washed, and dried under vacuum at 40 °C before the new run with fresh HMF solution. Upon recycling of the bismuth-promoted Pt/TiO₂ catalyst, only a slight decrease in the catalytic performance was observed. As expected, the deactivation was much less important for the bimetallic catalyst with respect to the loss of activity observed if monometallic Pt/TiO₂ catalyst was reused without pre-reduction. The recyclability of the catalyst has been much improved by Bi promotion, in accordance with previous studies on the increased resistance of Pt–Bi/C to oxygen poisoning. In all of the experiments presented in Figure 9, no Pt or Bi could be detected in the final reaction medium within the limits of the analysis method, which demonstrates also the chemical stability of the used catalyst. The small decrease in activity of the reused bimetallic catalyst still observed could be ascribed to deposition of some insoluble humins formed during the reaction. However, TGA measurements on the final used catalyst did not reveal any significant weight loss (Figure 4). Therefore, it could be the result of some overoxidation of the Pt particles despite the presence of Bi. Nevertheless, this loss of activity is much less than on the monometallic catalyst. The catalyst may recover its activity by reactivation under H₂, as was observed for the monometallic catalyst (Figure 7). In conclusion, as in the case of Pt/C catalysts, promotion by Bi decreases both oxidation and leaching of Pt under aerobic conditions.

Conclusions

TiO₂- and ZrO₂-based supported Pt catalysts were characterized and studied in the oxidation of HMF to FDCA in alkaline aqueous

solutions (NaHCO₃ or Na₂CO₃) with dioxygen from air. Preliminary investigations over Pt/TiO₂ showed that, if the reaction was carried out without addition of a homogeneous base, the reaction was blocked because the pH value became too acidic and precipitation of the carboxylic products formed occurred on the catalyst. In moderately alkaline aqueous solutions, the Pt-based catalyst became much more efficient. DFF and HMFCa were formed in a first step and further converted into FFCA and finally to FDCA with very good yields. The oxidation of the aldehyde moiety in FFCA is the limiting step under the given conditions, in accordance with the underlying mechanism (preliminary hydration step of the aldehyde function to form the geminal diol favored by the basic medium). We showed that the replacement of 4 equivalents of weak base NaHCO₃ by 2 equivalents of the stronger Na₂CO₃ base gave a catalytic system that was more active for the consecutive transformation of the FFCA intermediate to the fully oxidized FDCA. However, some byproducts were formed, which lowered the final yield of FDCA. A kinetic model was proposed based on the main reactions and major reaction components to predict the concentration–time trends reasonably well. In addition, promotion of Pt/TiO₂ by Bi displayed a catalyst with increased activity and ability for reuse. The Pt/ZrO₂ catalyst was slightly less active than Pt/TiO₂ under the optimized conditions. Introduction of Y₂O₃ or La₂O₃ in the ZrO₂ support did not show a cooperative effect of the weak basic sites in the solid and the homogeneous base.

Experimental Section

Catalyst preparation

The platinum-based catalysts were prepared with commercially available supports: TiO₂ (DT51, supplied by Millenium, now Cristal), ZrO₂, ZrO₂–10%La₂O₃, and ZrO₂–8%Y₂O₃ (MELCAT XZO, supplied by Mel Chemicals). The Mel Chemicals powders were pretreated by calcination in air (flow rate: 20 mL min^{–1}) at $T = 560\text{ }^{\circ}\text{C}$ for 3 h with a heating rate of 3 °C min^{–1}. The monometallic Pt catalysts were prepared by using a deposition–precipitation method in an aqueous solution of potassium tetrachloroplatinate.^[43] The support was slurried with water, and a desired amount of K₂PtCl₄ was added to this suspension. Afterwards, the pH value was adjusted to 11 by addition of solid KOH. The suspension was heated to reflux at a temperature of 80 °C for 1 h, after which the mixture was cooled and filtered. The solid was washed, dried, reduced under a hydrogen flow (flow rate: 60 mL min^{–1}; heating rate: 2 °C min^{–1} up to $T = 300\text{ }^{\circ}\text{C}$; $t = 3\text{ h}$ at $T = 300\text{ }^{\circ}\text{C}$) after purging with Ar, and finally passivated in 1% O₂/N₂.^[44,45]

To ensure the deposition of bismuth on the platinum, the bimetallic Pt–Bi catalysts were prepared through a surface redox reaction in the liquid phase from the monometallic catalysts and an aqueous solution of BiONO₃ with glucose as the reducing agent and according to a previously reported procedure.^[43,44] The monometallic Pt catalyst was added to an aqueous solution of glucose. An appropriate amount of BiONO₃ dissolved in 1 M HCl was added into the mixed slurry under a nitrogen atmosphere and the pH value was increased to 9 with NaOH. The catalyst was filtered, washed, and dried under vacuum at $T = 40\text{ }^{\circ}\text{C}$.

Catalyst characterizations

The platinum and bismuth contents in the solids were determined after digestion and dissolution of the solids in H_2SO_4 and aqua regia at $T=250\text{--}300^\circ\text{C}$ and analysis of the solution by using ICP-OES (Activa Jobin–Yvon).

The specific surface area (S_{BET}) was measured by N_2 adsorption/desorption at the liquid nitrogen temperature by using a Micromeritics 2020 apparatus after first degassing the sample under vacuum at $T=350^\circ\text{C}$ for 3 h.

Powder X-ray diffraction patterns were obtained with a D8 Advance A25 diffractometer (Bruker) with $\text{Cu}_{\text{K}\alpha}$ radiation ($\lambda=0.154184\text{ nm}$). The crystalline phases were identified by reference to the JCPDS (International Centre for Diffraction Data) data files. Crystal size values were calculated if possible by using the Scherrer equation from the width at half-maximum intensity.

TEM analysis of the supported catalysts was carried out with a JEOL 2010 microscope with a LaB6 source operating at 200 kV. The sample was suspended in ethanol and agitated ultrasonically. A drop of the suspension was placed on a copper mesh grid with carbon film coating, and the ethanol was allowed to evaporate. For the $\text{La}_2\text{O}_3\text{--ZrO}_2$ and $\text{Y}_2\text{O}_3\text{--ZrO}_2$ supported catalysts, extractive replica were used. A drop of the suspension was deposited on freshly cleaved mica, dried, and covered by a carbon film. After dissolution of the support in a solution of water, acetone, and HF, the metal particles remained stuck to the carbon film. The mean size of the nanoparticles was estimated by counting approximately 300–500 particles.

Catalytic experiments

HMF was purchased from Interchim as a 500 g batch of 95% purity. For all experiments described, the same batch was used without any purification. HMF contains impurities that were not identified; however, they are often reported as humins, which give some yellow color to the HMF substrate. Some of the dark humins formed during the preparation of HMF were shown to deposit on the catalyst surface and to deactivate the catalyst.^[46,47] The HPLC calibration was performed with HMF of higher purity (Sigma–Aldrich, >99%). The aqueous-phase reactions were performed in a 300 mL batch high-pressure reactor made of Hastelloy and equipped with a magnetically driven gas-inducing stirrer. In the standard reaction, HMF (95%; 2 g) dissolved in the alkaline aqueous solution (150 mL) containing the desired amount of base (expressed as the base/HMF molar ratio) was loaded into the reactor with an appropriate amount of catalyst (HMF/Pt molar ratio = 100). The initial concentration was chosen to be low because of the low solubility of the product acids HMFCa, FFCA, and FDCA in aqueous solution, which may cause precipitation and/or inhibit the reaction. The reactor was then sealed and pressurized with $P=40\text{ bar}$ air at time zero. The mixture was heated to the reaction temperature of 100°C (total pressure in the reactor then reached approximately 51 bar) under stirring (approximately 1000 rpm). The progress of the reaction was followed by taking liquid samples at regular times through a sample diptube. The samples were filtered (through a $0.45\text{ }\mu\text{m}$ polyvinylidene fluoride membrane), diluted 15 times, and then analyzed. After the reaction, the autoclave was cooled to room temperature and the catalyst was filtered off.

The progress of the reaction was determined by HPLC equipped with a photodiode array detector and a refractive index detector in series. The reaction products were separated on an ICE-Coragel 107H column thermostatted at $T=65^\circ\text{C}$, by using $10\text{ mM H}_2\text{SO}_4$ as the mobile phase at a fixed flux of 0.6 mL min^{-1} . Retention times and calibration curves for the observed products were

determined by injecting known concentrations of reference commercial products. The total organic carbon in solution was measured with a TOC analyzer (Shimadzu 5050A), and the measured value was compared to the molar balance calculated from HPLC analysis. The pH value was measured with a MeterLab PHM 240 pH meter.

The possible presence of platinum or bismuth in the reaction medium during the catalytic reactions was detected by ICP-OES of the liquid samples.

Acknowledgements

This work was supported by FUI (Fonds unique interministériel), FEDER (Fonds européen de développement régional), Conseil Régional de Picardie, and Conseil Régional de la Réunion within the PENTOVAl project. We thank the scientific services of IRCÉLYON for ICP-OES, XRD, and TEM analysis.

Keywords: biomass · bismuth · oxidation · platinum · supported catalysts

- [1] P. Gallezot, *Chem. Soc. Rev.* **2012**, *41*, 1538–1558.
- [2] M. Besson, P. Gallezot, C. Pinel, *Chem. Rev.* **2014**, *114*, 1827–1870.
- [3] T. Werpy, G. Petersen, *Top Value Added Chemicals from Biomass*, NREL/TP-510-35523, National Renewable Energy Laboratory, Golden, CO, **2004**.
- [4] J. J. Bozell, G. R. Petersen, *Green Chem.* **2010**, *12*, 539–554.
- [5] C. Moreau, M. N. Belgacem, A. Gandini, *Top. Catal.* **2004**, *27*, 11–30.
- [6] A. Gandini, D. Coelho, M. Gomes, B. Reis, A. Silvestre, *J. Mater. Chem.* **2009**, *19*, 8656–8664.
- [7] R.-J. van Putten, J. C. van der Waal, E. de Jong, C. B. Rasrendra, H. J. Heeres, J. G. de Vries, *Chem. Rev.* **2013**, *113*, 1499–1597.
- [8] Report by Grand View Research, Inc., “Furandicarboxylic Acid (FDCA) Market Potential Analysis And Segment Forecasts To 2020”, available from <http://www.grandviewresearch.com/industry-analysis/FDCA-Industry>.
- [9] A. A. Rosatella, S. P. Simeonov, R. F. M. Frade, C. A. M. Afonso, *Green Chem.* **2011**, *13*, 754–793.
- [10] R. Lopes de Souza, H. Yu, F. Rataboul, N. Essayem, *Challenges* **2012**, *3*, 212–232.
- [11] J. Lewkowsky, *Arkivoc* **2001**, 17–54.
- [12] W. Partenheimer, V. V. Grushin, *Adv. Synth. Catal.* **2001**, *343*, 102–111.
- [13] A. J. J. E. Eerhart, A. P. C. Faaij, M. K. Patel, *Energy Environ. Sci.* **2012**, *5*, 6407–6422.
- [14] P. Vinke, W. van der Poel, H. van Bekkum, *Stud. Surf. Sci. Catal.* **1991**, *59*, 385–394.
- [15] P. Verdegue, N. Merat, A. Gaset, *J. Mol. Catal.* **1993**, *85*, 327–344.
- [16] M. A. Lilga, R. T. Hallen, M. Gray, *Top. Catal.* **2010**, *53*, 1264–1269.
- [17] H. Ait Rass, N. Essayem, M. Besson, *Green Chem.* **2013**, *15*, 2240–2251.
- [18] Y. Y. Gorbanev, S. Kegnaes, A. Riisager, *Top. Catal.* **2011**, *54*, 1318–1324.
- [19] Y. Y. Gorbanev, S. Kegnaes, A. Riisager, *Catal. Lett.* **2011**, *141*, 1752–1760.
- [20] N. K. Gupta, S. Nishimura, A. Takagaki, K. Ebitani, *Green Chem.* **2011**, *13*, 824–827.
- [21] O. Casanova, S. Iborra, A. Corma, *ChemSusChem* **2009**, *2*, 1138–1144.
- [22] S. E. Davis, M. S. Ide, R. J. Davis, *Green Chem.* **2013**, *15*, 17–45.
- [23] Y. Y. Gorbanev, S. K. Klitgaard, J. M. Woodley, C. H. Christensen, A. Riisager, *ChemSusChem* **2009**, *2*, 672–675.
- [24] S. Davis, L. R. Houk, E. C. Tamargo, A. K. Datye, R. J. Davis, *Catal. Today* **2011**, *160*, 55–60.
- [25] T. Pasini, M. Piccinini, M. Blosi, R. Bonelli, S. Albonetti, N. Dimitratos, J. A. Lopez-Sanchez, M. Sankar, Q. He, C. J. Kiely, G. J. Hutchings, F. Cavani, *Green Chem.* **2011**, *13*, 2091–2099.
- [26] S. Albonetti, T. Pasini, A. Lolli, M. Blosi, M. Piccinini, N. Dimitratos, J. A. Lopez-Sanchez, D. J. Morgan, A. F. Carley, G. J. Hutchings, F. Cavani, *Catal. Today* **2012**, *195*, 120–126.

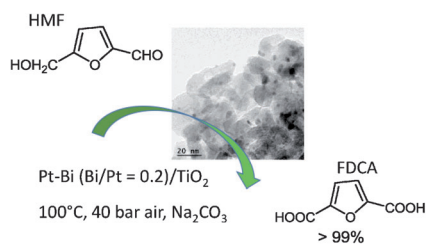
- [27] A. Villa, M. Schiavoni, S. Campisi, G. M. Veith, L. Prati, *ChemSusChem* **2013**, *6*, 609–612.
- [28] B. N. Zope, S. E. Davis, R. J. Davis, *Top. Catal.* **2012**, *55*, 24–32.
- [29] S. Siankevich, G. Savoglidis, Z. Fei, G. Laurenczy, D. T. L. Alexander, N. Yan, P. J. Dyson, *J. Catal.* **2014**, *315*, 67–74.
- [30] X. Wan, C. Zhou, J. Chen, W. Deng, Q. Zhang, Y. Yang, Y. Wang, *ACS Catal.* **2014**, *4*, 2175–2185.
- [31] B. Saha, D. Gupta, M. M. Abu-Omar, A. Modak, A. Bhaumik, *J. Catal.* **2013**, *299*, 316–320.
- [32] B. Siyo, M. Schneider, M.-M. Pohl, P. Langer, N. Steinfeldt, *Appl. Catal. A* **2014**, *478*, 107–116.
- [33] S. E. Davis, A. D. Benvidez, R. W. Gosselink, J. H. Bitter, K. P. de Jong, A. K. Datye, R. J. Davis, *J. Mol. Catal. A* **2014**, *388–389*, 123–132.
- [34] M. Besson, P. Gallezot in *Fine Chemicals through Heterogeneous Catalysis* (Eds.: R. A. Sheldon, H. van Bekkum), Wiley-VCH, Weinheim, **2001**, pp. 491–518.
- [35] T. Mallat, A. Baiker, *Chem. Rev.* **2004**, *104*, 3037–3058.
- [36] S. E. Davis, B. N. Zope, R. J. Davis, *Green Chem.* **2012**, *14*, 143–147.
- [37] K. R. Vuyyuru, P. Strasser, *Catal. Today* **2012**, *195*, 144–154.
- [38] I. van Zandvoort, Y. Wang, C. B. Rasrenda, E. R. H. van Eck, P. C. A. Bruijninx, H. J. Heeres, B. M. Weckhuysen, *ChemSusChem* **2013**, *6*, 1745–1758.
- [39] S. Subbiah, S. P. Simeonov, C. A. M. Afonso, *Green Chem.* **2013**, *15*, 2849–2853.
- [40] V. L. Snoeyink, D. Jenkins, *Water Chemistry*, Wiley, New York, **1990**, p. 462.
- [41] T. Caillot, Z. Salama, N. Chanut, F. J. Cadete Santos Aires, S. Benicci, A. Auroux, *J. Solid State Chem.* **2013**, *203*, 79–85.
- [42] T. Viinikainen, H. Rönkkönen, H. Bradshaw, H. Stephenson, S. Airaksinen, M. Reinikainen, P. Simell, O. Krause, *Appl. Catal. A* **2009**, *362*, 169–177.
- [43] R. Zanella, L. Delannoy, C. Louis, *Appl. Catal. A* **2005**, *291*, 62–72.
- [44] M. Besson, F. Lahmer, P. Gallezot, P. Fuertes, G. Fleche, *J. Catal.* **1995**, *152*, 116–121.
- [45] A. B. Crozon, M. Besson, P. Gallezot, *New J. Chem.* **1998**, *22*, 269–273.
- [46] S. P. Teong, G. Yi, X. Cao, Y. Zhang, *ChemSusChem* **2014**, *7*, 2120–2126.
- [47] G. Yi, S. P. Teong, X. Li, Y. Zhang, *ChemSusChem* **2014**, *7*, 2131–2137.

Received: December 10, 2014

Published online on ■ ■ ■ ■, 0000

FULL PAPERS

Back to bases: The addition of increasing amounts of NaHCO_3 soluble base improved significantly the catalytic activity of Pt/TiO_2 in HMF oxidation to FDCA by accelerating the oxidation rate of the aldehyde group. Moreover, the promotion of the catalyst with bismuth yielded a $\text{Pt-Bi}/\text{TiO}_2$ catalytic system (with Na_2CO_3 as the weak base) with improved activity and stability with respect to the monometallic catalyst.



H. Ait Rass, N. Essayem, M. Besson*



Selective Aerobic Oxidation of 5-HMF into 2,5-Furandicarboxylic Acid with Pt Catalysts Supported on TiO_2 - and ZrO_2 -Based Supports

